

# Performance comparison of interferometer topologies for carrier-envelope phase detection

C. Grebing · S. Koke · B. Manschwetus · G. Steinmeyer

Received: 26 August 2008 / Revised version: 13 November 2008 / Published online: 5 March 2009  
© Springer-Verlag 2009

**Abstract** Performance and noise immunity of different interferometer set-ups for carrier-envelope phase detection are compared. The frequently used Mach–Zehnder interferometer is found to be easily corrupted by acoustic noise contributions and air streaks, whereas a quasi-common-path variant of the  $f$ -to- $2f$  interferometer exhibits a 40% reduction of residual noise. This comparative analysis also provides deeper insight into additional mechanisms that are currently limiting the performance of carrier-envelope phase stabilization schemes.

PACS 42.65.Re · 07.60.Ly

## 1 Introduction

Measurement and stabilization of the carrier envelope phase (CEP) drift of femtosecond pulse trains has found widespread application in frequency metrology [1] and high-field nonlinear optics. One of the major achievements of CEP control of femtosecond laser pulses is the generation of isolated attosecond laser pulses [2] enabled by the precise timing control of the field maximum within the envelope structure of few-cycle laser pulses. Measurement and stabilization of the CEP drift of femtosecond oscillators relies on the  $f$ -to- $2f$  interferometer that heterodynes frequency-doubled long-wavelength components with fundamental components from the short-wavelength edge of

a frequency comb [3]. The first demonstrations of the  $f$ -to- $2f$  interferometer utilized a Mach–Zehnder (MZ)-type set-up, see, e.g., [4], a topology that has probably found the most widespread application, in particular in commercial devices. Since the MZ geometry is difficult to miniaturize and its rather large arm lengths are quite susceptible to acoustic noise, air streaks, and thermal drift, some authors have resorted to a Michelson-type geometry [5]. However, it appears difficult to reduce the arm lengths to below 1 cm for any kind of two-path interferometer. Moreover, it was recently reported that spurious interferometer noise may contribute to nearly half of the residual phase drift of a stabilized amplifier system [6]. This finding explains to some extent why in-loop measurements often appear to indicate 10 times smaller CEP noise values than an out-of-loop characterization [7]. Consequently, a more stable setup of the interferometer appears crucial for achieving better CEP stabilization. The issue of interferometer noise is easily avoided by an inline arrangement or common-path interferometer. While this concept is common-place for measurement of the CEP for amplified kHz-repetition rate laser systems [8], common-path arrangements for oscillator stabilization [9] only found application in fiber lasers [13, 14] and were applied to other laser systems essentially by only one group [10–12]. The major obstacle for using an inline geometry is the group delay between the  $f$  and the  $2f$  component, induced by dispersion of the set-up. For using heterodyne detection, it either has to be on the order of the pulse width [15], or it needs to be compensated. In particular, when microstructured fibers are used for spectral broadening, the  $f$ -to- $2f$  group delay easily amounts to picoseconds, requiring several thousand fs<sup>2</sup> for its compensation. In the following, we will show that group delay dispersion can be compensated in a quasi-common-path interferome-

C. Grebing (✉) · S. Koke · B. Manschwetus · G. Steinmeyer  
Max-Born-Institut für Nichtlineare Optik und  
Ultrakurzzeitspektroskopie, Max-Born-Straße 2a, 12489 Berlin,  
Germany  
e-mail: [grebing@mbi-berlin.de](mailto:grebing@mbi-berlin.de)

ter [9, 12], combining the noise immunity of true inline interferometers with the versatility of two-path interferometers.

## 2 Setup and results

For a systematic comparison of the noise sensitivity of different interferometers, we employ a commercial 88 MHz Ti:sapphire laser oscillator with 10-fs pulse duration and broaden its output in a 15-cm-long microstructure fiber. Given the group delay difference accumulated during this nonlinear interaction, fundamental and harmonics are temporally separated by about 1.5 ps. In the quasi-common-path (QCP) set-up shown in Fig. 1, compensation of this relatively large delay is accomplished by spatial separation of the spectral components that is achieved by a heavy-flint Brewster prism sequence with 17 cm apex separation. The sequence is arranged to separate infrared portions at 1060 nm and portions of the continuum at the second harmonic wavelength of 530 nm. The infrared and visible light are then separately retroreflected under a small vertical angle by a bisected end mirror. We find that a path difference of 4 mm is needed to compensate for the group delay differences generated in the microstructure fiber. The total unshared path between prism and retroreflector was about 55 mm. The bisected mirror is the only optical element that both arms do not share. All other components are passed commonly. The retroreflected beam is focused by an  $f = 18$  mm lens into a periodically poled lithium niobate crystal (PPLN), optimized for efficient 1060 nm frequency doubling. The generated 530 nm light is filtered out and detected by an avalanche photo diode (see QCP1 in Fig. 1). The signal of the avalanche photo diode is then fed into the

locking electronics, stabilizing the CEP drift to a quarter of the laser's repetition rate.

For comparison, a conventional Mach–Zehnder-type interferometer is also set up (see Fig. 1). Here fundamental and harmonics are split into the two interferometer arms by a dichroic mirror. Subsequently, frequency doubling and adjustment of the temporal delay is easily realized in separate arms. As already pointed out, the distinct spatial separation of both arms and the great number of optical elements not shared commonly by both arms renders the Mach–Zehnder setup sensitive to external perturbations, e.g., air streaks and vibrations caused by pumps and water chillers in the lab. Nevertheless, we tried to keep the separated beam paths to a minimum value of about 20 cm.

For an objective evaluation of the residual phase noise performance, we employ the out-of-loop measurement scheme depicted in Fig. 1. This scheme essentially consists of two interferometers: one for generating the signal for the feedback loop and a second one for an independent check of the CEP drift rate. In our setup we always apply a QCP interferometer (QCP1) as the in-loop interferometer. We then conduct the out-of-loop measurement with either an additional QCP interferometer (QCP2) or an MZ interferometer. In each of these interferometers we obtain a comparable beat note signal level of approximately 30 dB above the noise floor (resolution bandwidth = 100 kHz). Furthermore, we deliberately eliminate possible additional CEP noise contributions from the MSF by deriving the two beams for the in-loop and out-of-loop interferometer after the MSF. This ensures an exclusive comparison of the interferometer drifts in the MZ and QCP setup.

In the following we show and analyze the CEP drift time series of the out-of-loop interferometer as obtained from a radio-frequency lock-in measurement. For a first demonstration, we removed the enclosures of the out-of-loop interferometers and operated them without shielding them against acoustics and air movements. The considerably better performance of the QCP geometry is obvious from the out-of-loop phase error shown in Fig. 2(a). While the MZ setup displays a pronounced drift and strong phase excursions, the QCP setup exhibits no drift. This results in a three times larger rms standard deviation of 1.58 rad for the MZ setup compared to a value of 550 mrad for the QCP geometry. A detailed analysis of the phase noise frequency dependence is shown in Fig. 2(b). In the unshielded case there is nearly no difference in the broad acoustic noise band in the region between 100 and several 1000 Hz, whereas the two curves diverge for frequencies below 100 Hz. This divergence is due to the slow drifts already observed in the time series. In consequence, this test confirms the anticipated improved immunity towards air streaks of the QCP geometry owing to commonly shared optical paths and elements.

In a second experiment, we eliminated the external disturbances by enclosing the out-of-loop interferometer and

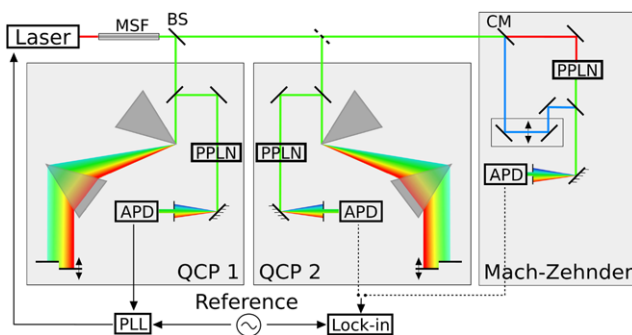


**Fig. 1** Illustration of the measurement setup. MSF: microstructure fiber for spectral broadening. PPLN: periodically poled lithium niobate for second harmonic generation of 1060 nm. APD: avalanche photodiode for detecting the beat signal. PLL: phase locked loop. CM: cold mirror. BS: beam splitter. The prisms are separated by about 15 cm in order to achieve the required spatial separation. Furthermore, splitting of the incoming and retroreflected beam is obtained by a bisected end mirror that is slightly tilted vertically

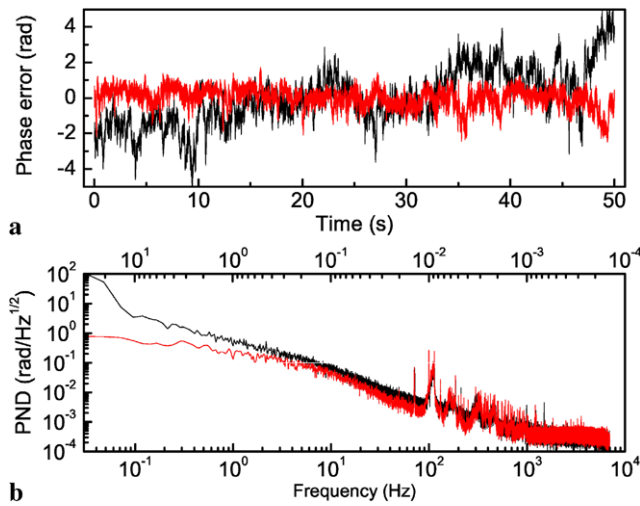


**Fig. 2** Measurement results, unshielded mode. *Red*: QCP, *black*: MZ. (a) Phase error vs. observation time. Residual rms phase noise: 1.58 rad (MZ), 550 mrad (QCP). (b) Phase noise density vs. frequency and observation time

reidid the measurements. The time series of the phase noise measured out-of-loop with both the MZ and QCP setups are shown in Fig. 3(c). Additionally, we also recorded the error voltage of the phase locked loop and evaluated the in-loop CEP noise. As already reported by others [7], the in-loop standard deviation underestimates the out-of-loop values by almost one order of magnitude. This discrepancy corroborates the necessity of out-of-loop measurements for a reliable evaluation of the residual CEP drift.

A comparison of the out-of-loop time series reveals the better performance of the QCP geometry, which immediately results in a >40% reduced residual CEP noise of 150 mrad compared to the MZ setup. Spectrally analyzing the phase noise (Fig. 3(b)), we mainly observe a noise reduction in the acoustic band above 100 Hz. This difference becomes clearer when looking at the integrated phase noise depicted in Fig. 3(a). In this representation, the phase noise density is integrated from the sampling rate to the inverse observation time  $1/\Delta t$ , showing the contributions of the peaks in Fig. 3(b) to the rms noise as pronounced steps at about 95, 100, 400, 800, and 900 Hz. The strongest of these steps appears in both traces with nearly equal 110 mrad magnitude, while all other steps appear only in the MZ trace and exhibit a step height of about 10 mrad. We therefore attribute the smaller steps in this region to forced mirror vibrations caused by acoustic noise in the lab, which affect the MZ setup more strongly than the QCP. It is readily calculated that, in the wavelength region of interest, a step height of about 10 mrad corresponds to tiny mirror displacements of less than 1 nm rms. Alternatively, the different noise susceptibility of the different interferometers may also be explained by air streaks in the interferometers, i.e., small induced beam deflections resulting from

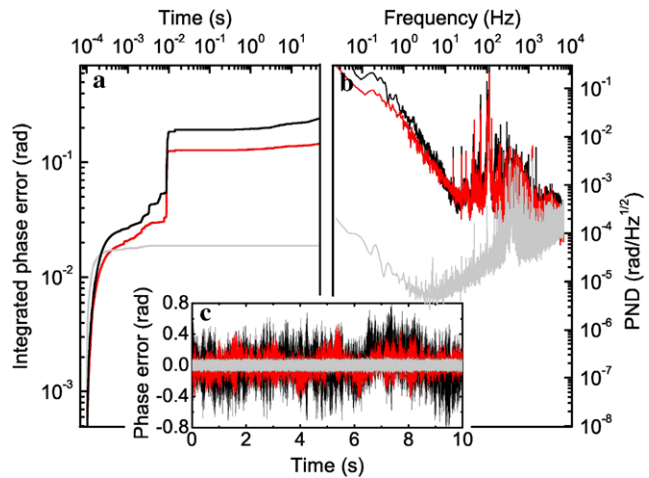


**Fig. 3** Measurement results, shielded mode. *Red*: QCP, *black*: MZ, gray: in-loop. (a) Integrated phase error vs. observation time. (b) Phase noise density vs. frequency. (c) 10 s segment of a 120 s long phase error time series. Residual rms phase noise over the entire time series: 240 mrad (MZ), 150 mrad (QCP), 20 mrad (in-loop)

a thermally or acoustically induced refractive index variations across the beam paths. These effects are particularly important for explaining the observed differences in Fig. 2. Concerning air streaks, numerical simulations indicate an about 100 times smaller sensitivity of a QCP setup with 2 mm beam separation compared to Michelson or Mach–Zehnder interferometers with otherwise equal arm lengths.

Apart from the acoustically induced distortions, the strongest step-like feature in Fig. 3(b), however, appears at an identical height of about 110 mrad at 100 Hz in both curves. The particular frequency and its appearance in both interferometers makes an acoustic origin very unlikely. We could trace the likely origin of this noise contribution back to residual power supply ripple of about 100 µV at 100 Hz in our commercial locking electronics. Theoretical elimination of this contribution caused by the power supply would reduce the residual phase noise to about 40 mrad, which is comparable to the in-loop value.

Finally, the integrated phase noise plots also show a slight increase for long observation time, which is again more pronounced for the MZ interferometer than for the QCP setup. This increase might indicate residual thermal interferometer drift still present in the shielded interferometers.

Our analysis clearly isolates the different contributions to the frequently observed discrepancy between in-loop and out-of-loop measurements. While acoustic pick-up of the MZ interferometer contributes to slightly less than half of the observed residual noise, elimination of the power supply ripple brings the residual jitter into the 30 mrad range, which constitutes nearly an order-of-magnitude improvement over previously reported values.

### 3 Conclusion

Our systematic comparison shows that a quasi-common-path  $f$ -to- $2f$  interferometer is clearly more immune towards acoustical noise and air streaks than the traditional Mach-Zehnder set-up. We observed a more than 40% reduction of the CEP noise. The QCP set-up is very simple to implement and certainly less complex than separate stabilization of the interferometer to a He-Ne laser, as recently suggested in [6]. Moreover, the set-up does not require a combining beam splitter, which allows for an increase of power levels on the detector of up to 3 dB. As the QCP interferometer involves only a small section that is not common path, some very small residual drift may exist. In principle, the small unshared path could also be completely eliminated using chirped mirrors instead of a prism assembly if the group delay difference accumulated in the MSF is small enough.

While the advantages of an improved locking performance are at hand for stabilizing amplifier systems, our method may also be advantageous for the field of frequency metrology. One of the current challenges is pushing the precision in frequency measurements which is necessary for detecting small possible drifts of the values of fundamental constants [16, 17]. Using a common-path interferometer for metrology applications may therefore serve to remove at least one problematic issue in this quest for precision.

**Acknowledgements** The authors acknowledge financial support from the Deutsche Forschungsgemeinschaft under grant STE 762/5-1.

### References

1. T. Udem, R. Holzwarth, T.W. Hänsch, *Nature (Lond.)* **416**, 233–237 (2002)
2. E. Goulielmakis, M. Uiberacker, R. Kienberger, A. Baltuška, V. Yakovlev, A. Scrinzi, T. Westerwalbesloh, U. Kleineberg, U. Heinzmann, M. Drescher, F. Krausz, *Science* **305**, 1267–1269 (2004)
3. H.R. Telle, G. Steinmeyer, A.E. Dunlop, J. Stenger, D.H. Sutter, U. Keller, *Appl. Phys. B* **69**, 327–332 (1999)
4. D.J. Jones, S.A. Diddams, J.K. Ranka, A. Stentz, R.S. Windeler, J.L. Hall, S.T. Cundiff, *Science* **288**, 635–639 (2000)
5. T.M. Fortier, A. Bartels, S.A. Diddams, *Opt. Lett.* **31**, 1011–1013 (2006)
6. E. Moon, C. Li, Z. Duan, J. Tackett, K.L. Corwin, B.R. Washburn, Z. Chang, *Opt. Express* **14**, 9758–9763 (2006)
7. T.M. Fortier, D.J. Jones, J. Ye, S.T. Cundiff, R.S. Windeler, *Opt. Lett.* **27**, 1436–1438 (2002)
8. M. Kakehata, H. Takada, Y. Kobayashi, K. Torizuka, Y. Fujihira, T. Homma, H. Takahashi, *Opt. Lett.* **26**, 1436–1438 (2001)
9. F.W. Helbing, Ph.D. Thesis, Swiss Federal Institute of Technology, Zürich, Switzerland (2004)
10. D.J. Jones, T.M. Fortier, S.T. Cundiff, *J. Opt. Soc. Am. B* **21**, 1098–1103 (2004)
11. T.M. Fortier, P.A. Roos, D.J. Jones, S.T. Cundiff, R.D.R. Bhat, J.E. Sipe, *Phys. Rev. Lett.* **92**, 147403 (2004)
12. I. Thomann, E. Gagnon, R.J. Jones, A.S. Sandhu, A. Lytle, R. Anderson, J. Ye, M. Murnane, H. Kapteyn, *Opt. Express* **12**, 3493–3499 (2004)
13. T.R. Schibli, K. Minoshima, F.-L. Hong, H. Inaba, A. Onae, H. Matsumoto, I. Hartl, M.E. Fermann, *Opt. Lett.* **29**, 2467–2469 (2004)
14. J.J. McFerran, W.C. Swann, B.R. Washburn, N.R. Newbury, *Opt. Lett.* **31**, 1997–1999 (2006)
15. J. Rauschenberger, T. Fuji, M. Hentschel, A.-J. Verhoeft, T. Udem, C. Gohle, T.W. Hänsch, F. Krausz, *Laser Phys. Lett.* **3**, 37–42 (2006)
16. J.K. Webb, M.T. Murphy, V.V. Flambaum, V.A. Dzuba, J.D. Barrow, C.W. Churchill, J.X. Prochaska, A.M. Wolfe, *Phys. Rev. Lett.* **87**, 091301 (2001)
17. M. Fischer, N. Kolachevsky, M. Zimmermann, R. Holzwarth, T. Udem, T.W. Hänsch, M. Abgrall, J. Grünert, I. Maksimovic, S. Bize, H. Marion, F. Pereira Dos Santos, P. Lemonde, G. Santarelli, P. Laurent, A. Clairon, C. Salomon, M. Haas, U.D. Jentschura, C.H. Keitel, *Phys. Rev. Lett.* **92**, 230802 (2004)